

Supporting Information for

H-ferritin–nanocaged gadolinium nanocores for ultra-sensitive MR molecular imaging

Jianlin Zhang^{1,2#}, Chang Yuan^{1#}, Lingfei Kong^{3#}, Feiyan Zhu¹, Wanzhong Yuan⁴, Junying Zhang¹, Juanji Hong¹, Tao Wang^{4*}, Zhentao Zuo^{5*}, Minmin Liang^{1*}

¹Experimental Center of Advanced Materials, School of Materials Science & Engineering, Beijing Institute of Technology, Beijing, 100081, China.

²Center of Basic Medical Research, Institute of Medical Innovation and Research, Peking University Third Hospital, Beijing, China.

³National Laboratory of Biomacromolecules, Institute of Biophysics, Chinese Academy of Sciences, Beijing, China.

*Correspondence to:

Tao Wang, MD. Email: wangtao@bjmu.edu.cn

Zhentao Zuo, PhD. Email: zuozt@ibp.ac.cn

Minmin Liang, PhD. Email: mmliang@bit.edu.cn

#These three authors contributed equally.

Contents

1. Supporting Figures	S2-7
2. Supporting Tables.....	S8-12

1. Supporting Figures

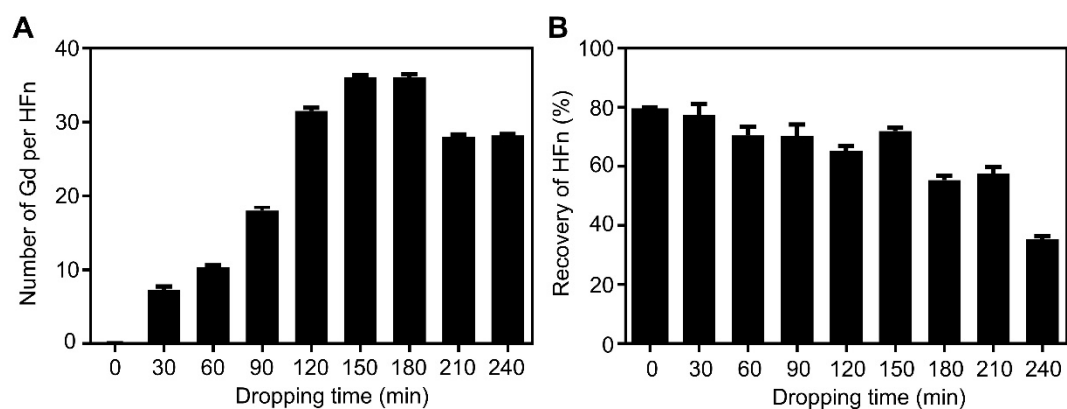


Figure S1. (A) Number of loaded Gd per HFn nanocage depends on the Gd dropping time. (B) HFn recovery yield (%) depends on the Gd dropping time. The encapsulated Gd was quantified using ICP-OES, and the HFn concentration was determined by using BCA protein assay kit.

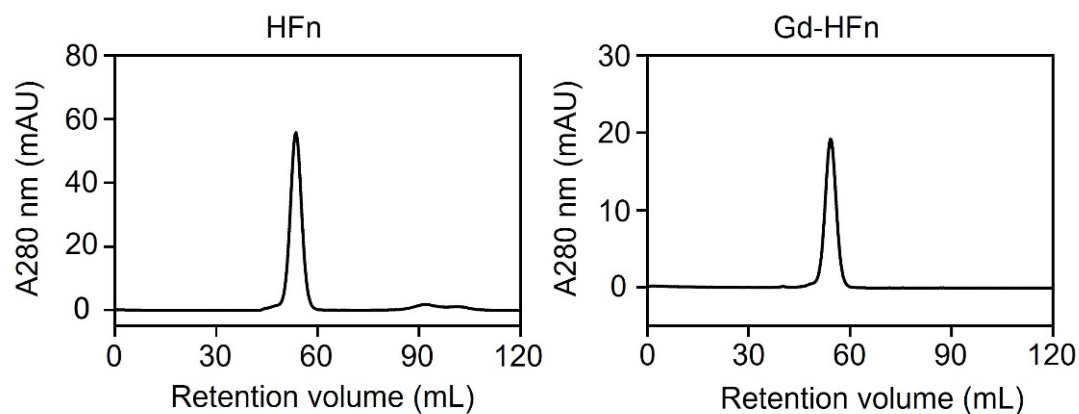


Figure S2. Representative SEC analysis of the HFn and Gd-HFn NPs.

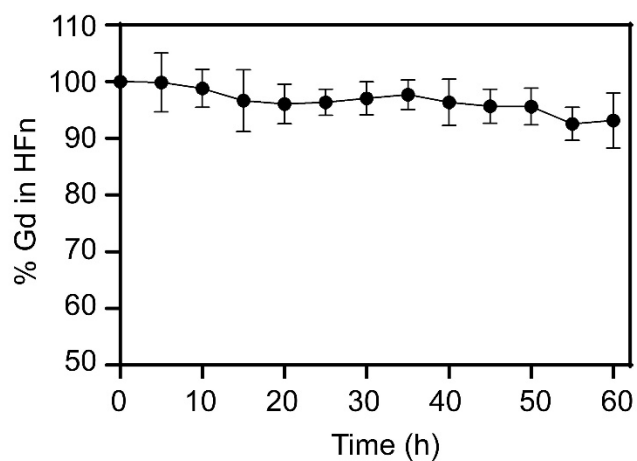


Figure S3. Stability of Gd-HFn NPs in 10% mouse serum at 37 °C over 60 h of incubation (n = 3, bars represent means \pm s.d.)

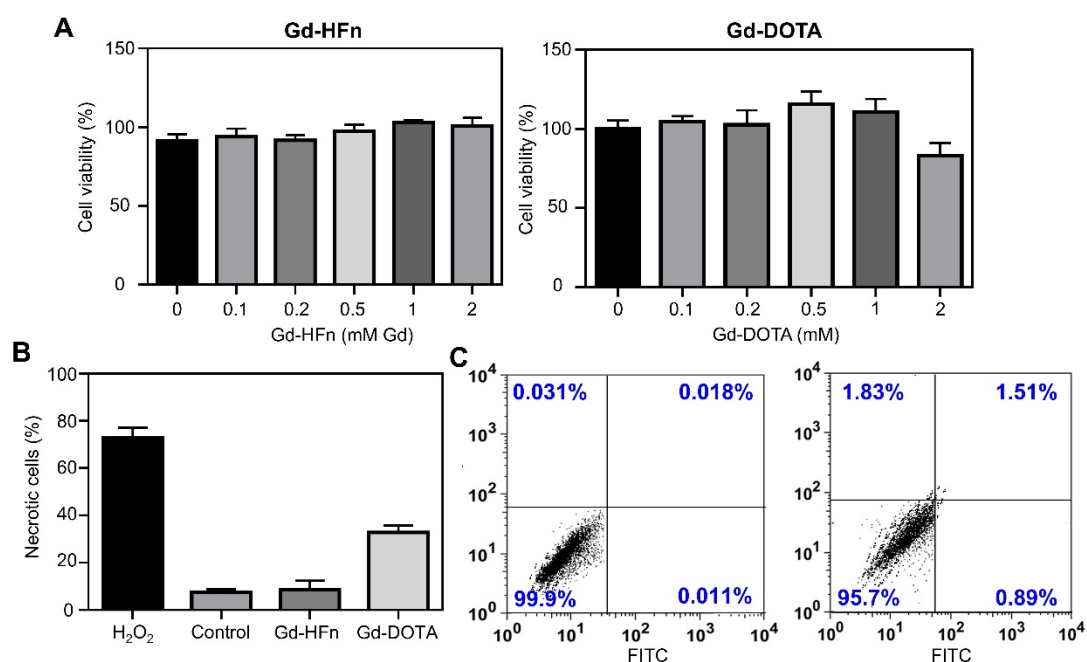


Figure S4. (A) Cell viability of MDA-MB-231 cells after treatment with Gd-HFn or Gd-DOTA for 24 h over a dose range of 0-2 mM Gd. CCK8 assay was used for cell viability assessment. (n = 5, bars represent means \pm s.d.) (B) The percentage of necrotic cells measured by quantification of LDH release in the cell medium after incubation in the presence or absence (Negative control) of Gd-HFn or Gd-DOTA (2 mM Gd). Hydrogen peroxide (H₂O₂) was used as positive control. Results are expressed as percentage of dead cells with respect to the control. (n = 5, bars represent means \pm s.d.) (C) Cell apoptosis analysis was performed using Annexin V-FITC assay using flow cytometry. Left, MDA-MB-231 cells untreated. Right, MDA-MB-231 cells treated with Gd-HFn for at concentration of 2 mM Gd.

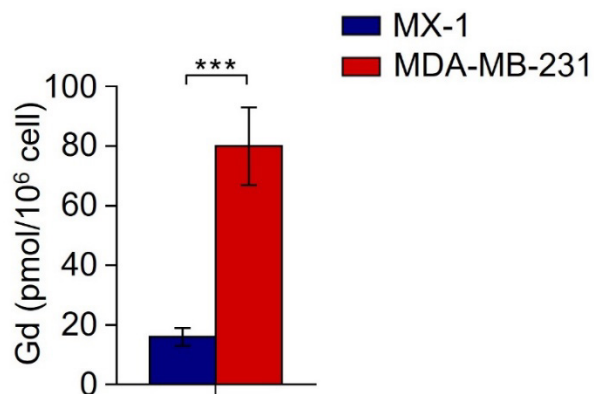


Figure S5. Cellular uptake of Gd-HFn measured by ICP-OES (n = 5, mean ± SD, unpaired Student's t-test, ***P < 0.001).

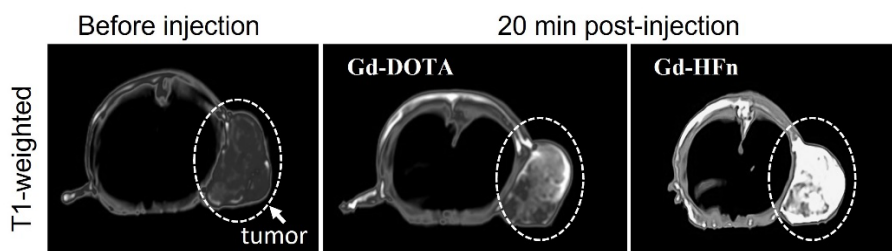


Figure S6. MR imaging of large tumors with Gd-DOTA or Gd-HFn in living mice.

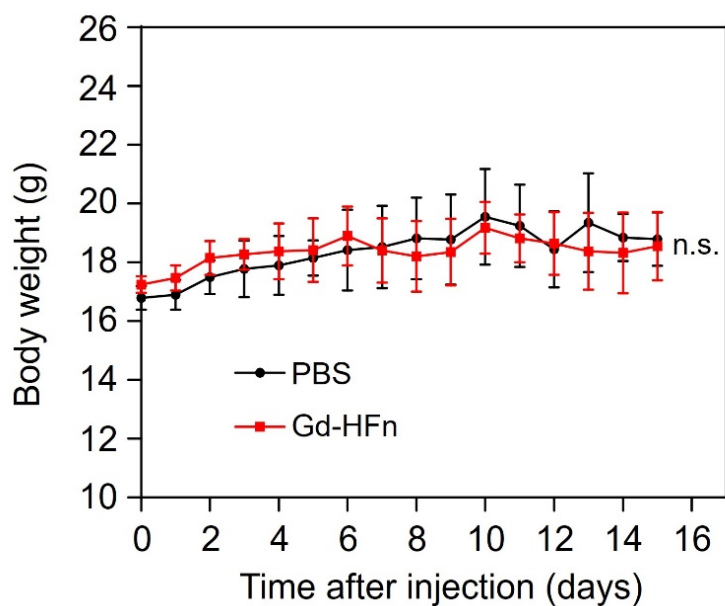


Figure S7. Toxicity evaluation of Gd-HFn *in vivo*. Healthy female BALB/c mice were administered intravenously on day 0 of Gd-HFn (0.016 mmol Gd/kg body weight) or PBS (n = 6 per group, bars represent means \pm s.d.). n.s., not significant.

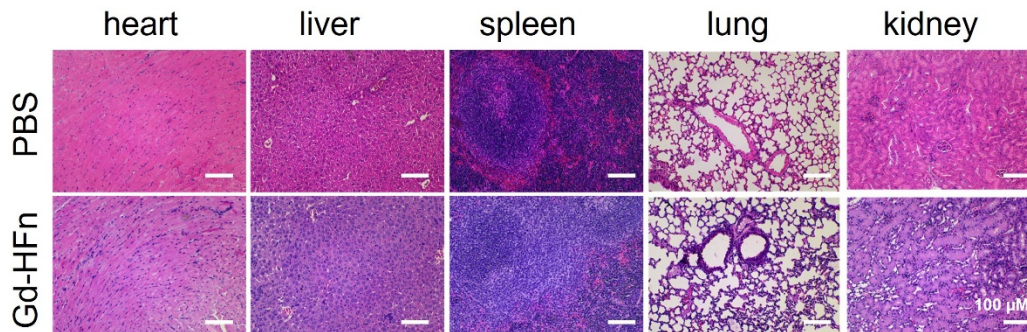


Figure S8. Representative images of organ histology examination from mice administered with PBS or Gd-HFn at a dose of 0.016 mmol Gd/kg animal body weight. Tissue slices were stained with hematoxylin and eosin (H&E). No noticeable abnormality was found in the heart, liver, spleen, lung, and kidney.

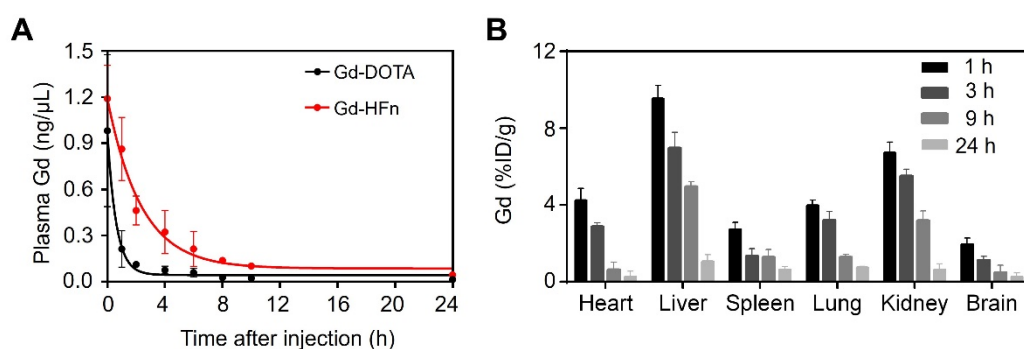


Figure S9. Total body clearance of Gd-HFn. (A) Plasma concentrations of Gd as a function of time after injection. Five healthy mice were intravenously injected with Gd-DOTA or Gd-HFn at a dose of 0.016 mmol Gd/kg animal body weight. Plasma samples at different time points were drawn and the plasma concentrations of Gd were measured by ICP-OES. (n=5 independent measurements, error bars represent mean \pm s.d.). (B) Biodistribution of Gd-HFn. Tissue samples at different time points were drawn and the tissue concentrations of Gd were measured by ICP-OES. Data are presented as percentage of injected dose (%ID) per gram of tissue. Values are expressed as means \pm s.d. for a group of five animals.

Table S1. Blood routine parameters of healthy mice treated with PBS, Gd-DOTA or Gd-HFn.

Blood routine parameters	PBS (n=5)		Gd-DOTA (n=5)		Gd-HFn (n=5)		Normal arrange
	1 Week	2 Weeks	1 Week	2 Weeks	1 Week	2 Weeks	
WBC	3.96±0.76	8.94±0.96	4.55±0.64	8.78±0.70	4.34±0.87	8.82±1.27	0.80-10.60
NEU	0.42±0.18	1.08±0.17	0.68±0.13	1.04±0.08	0.83±0.24	1.27±0.24	0.23-3.60
LYM	3.41±0.75	7.52±0.89	3.71±0.61	7.09±0.63	3.28±0.67	6.77±1.23	0.60-8.90
MON	0.06±0.01	0.25±0.05	0.09±0.01	0.36±0.04	0.10±0.02	0.31±0.07	0.04-1.40
EOS	0.05±0.02	0.24±0.09	0.06±0.01	0.23±0.04	0.11±0.06	0.21±0.07	0-0.51
BAS	0.01±0.00	0.05±0.01	0.02±0.01	0.05±0.02	0.02±0.01	0.06±0.02	0-0.12
NEU%	10.84±5.25	9.66±1.95	15.00±3.37	11.88±0.64	19.30±4.50	14.70±5.62	6.5-50.0
LYM%	85.72±5.24	85.38±3.44	81.30±3.64	80.70±1.29	75.40±4.99	78.84±6.38	40.0-92.0
MON%	1.58±0.33	2.30±0.71	1.92±0.23	4.14±0.26	2.38±0.47	3.46±1.08	0.9-18.0
EOS%	1.42±0.29	2.24±1.10	1.40±0.21	2.66±0.55	2.36±0.78	2.24±0.29	0-7.5
BAS%	0.44±0.08	0.42±0.07	0.38±0.13	0.62±0.20	0.56±0.16	0.76±0.27	0-1.5
RBC	9.62±0.35	9.17±0.43	9.57±0.23	8.86±0.51	9.07±0.61	8.97±0.43	6.50-11.50
HGB	152.20±3.60	148.60±6.41	150.80±5.78	144.80±7.55	142.40±7.66	145.20±4.79	110-165
HCT	46.24±1.76	44.30±1.73	46.30±1.36	43.78±2.29	43.52±2.42	43.78±1.39	35.0-55.0
MCV	48.06±0.62	48.32±0.54	48.38±0.47	49.46±0.57	48.04±0.86	48.82±1.03	41.0-55.0
MCH	15.84±0.22	16.22±0.25	15.74±0.31	16.38±0.40	15.76±0.27	16.24±0.27	13.0-18.0
MCHC	329.60±5.46	335.20±2.79	325.40±6.15	331.20±4.49	327.60±2.73	332.40±2.33	300-360

PLT	1051.40±129.5 6	1028.40±373.36	1055.00±118. 87	940.00±169. 35	1526.40±322.2 1	1190.80±168.04	400-1600
MPV	4.68±0.22	4.82±0.34	4.56±0.05	4.78±0.04	4.58±0.10	4.78±0.07	4.0-6.2
PDW	15.18±0.07	15.28±0.07	15.30±0.11	15.22±0.07	15.14±0.12	15.18±0.12	12.0-17.5
PCT	0.49±0.07	0.48±0.17	0.48±0.05	0.45±0.08	0.70±0.13	0.57±0.08	0.100- 0.780

Plasma samples were obtained 1 week and 2 weeks after treatment. WBC, white blood cell; NEU, neutrophil; LYM, lymphocyte; MON, monocyte; EOS, eosinophilic cell; BAS, basophil; RBC, red blood cell; HGB, hemoglobin; HCT, hematocrit; MCV, mean corpuscular volume; MCH, mean corpuscular hemoglobin; MCHC, mean corpuscular hemoglobin concentration; PLT, Platelets; MPV, mean platelet volume; PDW, platelet distribution width; PCT, thrombocytocrit.

Table S2 Comparison of the relaxivity values of Gd-HFn with the major Gd-based contrast agents reported in the literature.

Contrast agent	Structure	r_1 (mM ⁻¹ s ⁻¹)	r_2 (mM ⁻¹ s ⁻¹)	Refs	
Magnevist®	Gd-DTPA	3.9-4.3 (1.5 T)	3.8-5.4 (1.5 T)	[1,10]	
		3.5-3.9 (3 T)	4.3-6.1 (3 T)		
		3.5 ± 0.1 (1.4 T)	5.1 ± 0.2 (1.4 T)		
Omniscan®	Gd-DTPA-BMA	4.0-4.6 (1.5T)	4.2-6.2 (1.5 T)	[2]	
		3.8-4.2 (3T)	4.7-6.5 (3 T)		
ProHance®	Gd-DO3A-HP	3.9-4.3 (1.5 T)	4.2-5.8 (1.5 T)	[2,9]	
		3.5-3.9 (3 T)	4.8-6.6 (3 T)		
Dotarem®	Gd-DOTA	3.94 (0.25T)	3.4-5.2 (1.5 T)	[3,5,8,9]	
		2.96-3.8 (1.5 T)			4.0-5.8 (3 T)
		3.3-3.7 (3 T)			
Multihance®	Gd-BOPTA	2.85 (9.4)	7.8-9.6 (1.5 T)	[3]	
		6.0-6.6 (1.5 T)			10.0-12.0 (3 T)
		5.2-5.8 (3 T)			
OptiMARK®	Gd-DTPA-BMEA	4.4-5.0 (1.5 T)	4.3-6.1 (1.5 T)	[3]	
		4.2-4.8 (3 T)	5.0-6.8 (3 T)		
C-Cha-DOTA	(Gd ³⁺)-chelating 1,4,7,10- tetraazacyclododecane- 1,4,7,10-tetraacetic acid (DOTA)	19.5 (sphere), 17.2 (fiber)	/	[4]	
Ppdf-Gd	piX-PEG8- SSSPLGLAK (DOTA)-PEG6-F4	28.2 (sphere), 51.5 (fiber) (0.25 T)	/	[5]	
SMNs-Gd, FMNs-Gd	spherical micellar nanoparticles (Gd ³⁺), fibril-shaped micellar nanoparticles (Gd ³⁺)	15.6, 18.5 (0.5 T)	/	[6]	
ultrasmall gadolinium oxide	poly(acrylic acid-co- maleic acid) (PAAMA) -coated ultrasmall Gd ₂ O ₃	40.6 (3 T)	63.34 (3 T)	[7]	
PEG-P(Lys- DOTA-Gd)	the micelle-forming poly(ethylene glycol)-b-poly(lysine)	13.31 (1.5 T) 5.54 (9.4 T)	/	[8]	
Elucirem® (FDA approved in 2022)	Gadopicienol C ₃₅ H ₅₄ GdN ₇ O ₁₅	12.8 (1.4 T)	/	[9]	
		11.6 (3 T)			

GONP-12	Gd ₂ O ₃ -PAMPS-LA	63.0±4.4 (9.4 T)	73.5±2.4 (9.4 T)	[10]
Gadolinium Oxide Nanoparticles	PASA-coated Gd ₂ O ₃ nanoparticles	19.1 (3 T)	53.7 (3 T)	[11]
RGD2	ES-GON5-PAA@RGD2	68.7±2.3 (1.5 T) 19.9±0.8 (7 T)	70.5±1.6 (1.5 T) 54.8±2.7 (7 T)	[12]
AFt-C4 NPs	Gd(III) compound (C4) based on Apoferritin	3.3 (0.5 T)	/	[13]
Magnetoferritin	Protein-coated	8 (1.5 T)	218 (1.5 T)	[6]
The proposed MRI contrast agent	HF _n -Gd	549 (1.5 T) 428 (3 T)	1555 (1.5 T) 1286 (3 T)	This work

References:

1. Caravan P, Ellison J, McMurry T, Lauffer R. Gadolinium (III) chelates as MRI contrast agents: structure, dynamics, and applications. *Chem Rev*, 1999; 99(9): 2293-2352.
2. Hao D, Ai T, Goerner F, Hu X, Runge VM, Tweedle M. MRI contrast agents: basic chemistry and safety. *J Magn Reso Imaging*, 2012; 36(5): 1060-1071.
3. Yan GP, Robinson L, Hogg P. Magnetic resonance imaging contrast agents: overview and perspectives. *Radiography*, 2007; 13: e5-e19.
4. Kim I, Han EH, Ryu J, Min JY, Ahn H, Chung YH, et al. One-dimensional supramolecular nanoplateforms for theranostics based on co-assembly of peptide amphiphiles. *Biomacromolecules*, 2016; 17(10): 3234-3243.
5. Zhang J, Mu YL, Ma ZY, Han K, Han HY. Tumor-triggered transformation of chimeric peptide for dual-stage-amplified magnetic resonance imaging and precise photodynamic therapy. *Biomaterials*, 2018; 182: 269-278.
6. Randolph LM, LeGuyader CL, Hahn ME, Andolina CM, Patterson JP, Mattrey RF, et al. Polymeric Gd-DOTA amphiphiles form spherical and fibril-shaped nanoparticle MRI contrast agents, *Chem Sci*. 2016; 7(7): 4230-4236.
7. Jang YJ, Liu S, Yue H, Park JA, Cha H, Ho SL, et al. Hydrophilic biocompatible poly (acrylic acid-co-maleic acid) polymer as a surface-coating ligand of ultrasmall Gd₂O₃ nanoparticles to obtain a high r₁ value and T₁ MR images. *Diagnostics*, 2020; 11(1): 2.
8. Yokoyama M, Shiraishi K. Stability evaluation of Gd chelates for macromolecular MRI contrast agents. *Magn Reson Mater Phy, Biology and Medicine*, 2020; 33: 527-536.
9. Lancelot E, Raynaud JS, Desché P. Current and future MR contrast agents: seeking

- a better chemical stability and relaxivity for optimal safety and efficacy. *Invest Radiol*, 2020; 55(9): 578-588.
10. Stinnett G, Taheri N, Villanova J, Bohloul A, Guo X, Esposito EP, et al. 2D gadolinium oxide nanoplates as T1 magnetic resonance imaging contrast agents. *Adv Healthc Mater*, 2021; 10(11): 2001780.
 11. Marasini S, Yue H, Ghazanfari A, Ho SL, Park JA, Kim S, et al. Polyaspartic acid-coated paramagnetic gadolinium oxide nanoparticles as a dual-modal t1 and t2 magnetic resonance imaging contrast agent. *Applied Sciences*, 2021; 11(17): 8222.
 12. Shen Z, Fan W, Yang Z, Liu Y, Bregadze VI, Mandal SK, et al. Exceedingly small gadolinium oxide nanoparticles with remarkable relaxivities for magnetic resonance imaging of tumors. *Small*, 2019; 15(41): 1903422.
 13. Man X, Yang T, Li W, Li S, Xu G, Zhang Z, et al. Developing a gadolinium (III) compound based on apoferritin for targeted magnetic resonance imaging and dual-modal therapy of cancer. *J Med Chem*, 2023; 66(11): 7268–7279.